Supporting information

Co-VN encapsuled in bamboo-like N-doped carbon nanotubes for ultrahigh stability oxygen reduction reaction

Ying Wang,[a] Lei Wang,*[,b] Miaomiao Tong,[b] Xiaojun Zhao,[a] Yanting Gao,[a] Honggang Fu*[,b]

[a] Key Laboratory of Inorganic-Organic Hybrid Functional Material Chemistry, Ministry of Education, Tianjin Key Laboratory of Structure and Performance for Functional Molecules, College of Chemistry, Tianjin Normal University, Tianjin 300387, China.

[b] Key Laboratory of Functional Inorganic Material Chemistry, Ministry of Education of the People's Republic of China, Heilongjiang University, Harbin 150080, China.

Table S1. The synthetic conditions for all the compared samples.

samples	$Co(NO_3)_2 \cdot 6H_2O$ (mmol)	NH_4VO_3 (mmol)	Melamine (mmol)	Carbonized temperature (^oC)
NGT-$Co_{30}V_{70}$-45-900	1.14	2.66	45	900
NGT-$Co_{35}V_{65}$-45-900	**1.33**	**2.47**	**45**	**900**
NGT-$Co_{40}V_{60}$-45-900	1.52	2.28	45	900
NGT-$Co_{35}V_{65}$-45-800	1.33	2.47	45	800
NGT-$Co_{35}V_{65}$-45-1000	1.33	2.47	45	1000
NGT-$Co_{35}V_{65}$-30-900	1.33	2.47	30	900
NGT-$Co_{35}V_{65}$-35-900	1.33	2.47	35	900
NGT-$Co_{35}V_{65}$-40-900	1.33	2.47	40	900
NGT-$Co_{35}V_{65}$-50-900	1.33	2.47	50	900
NGT-Co-45-900	1.33	0	45	900
NC-V-45-900	0	2.47	45	900
NGT-V-45-900 (after acid treatment)	1.33	2.47	45	900

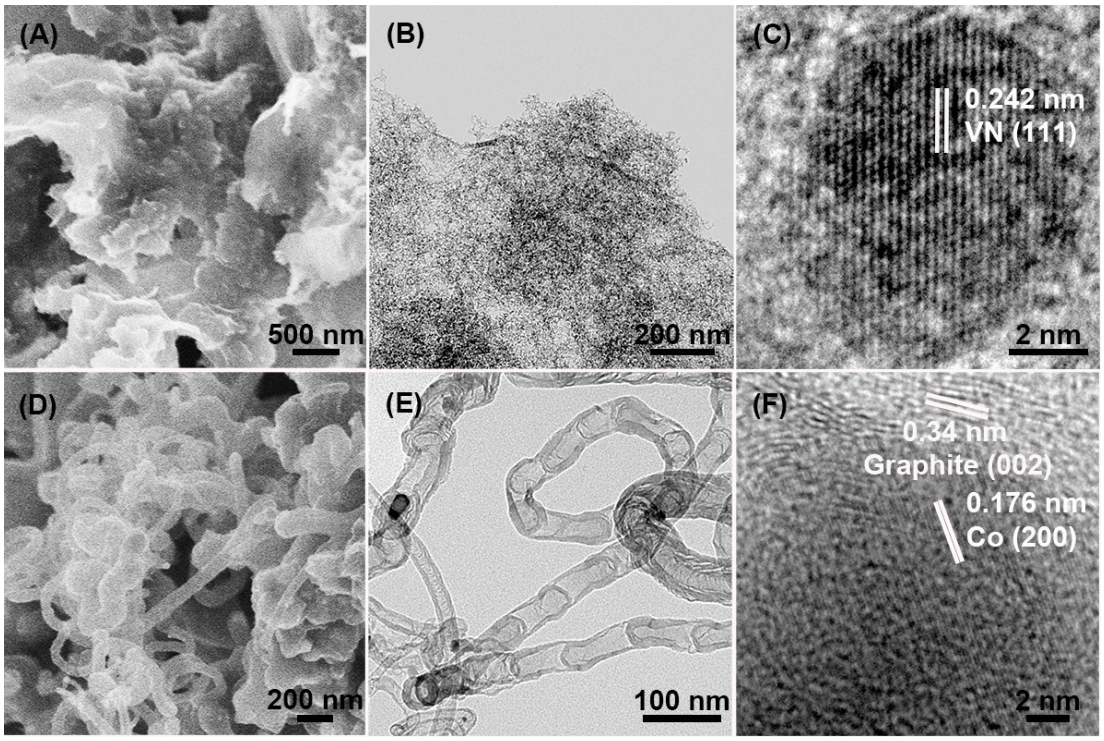

Fig. S1 (A) SEM, (B) TEM and (C) HRTEM images of NC-V-45-900. (D) SEM, (E) TEM and (F) HRTEM images of NGT-Co-45-900.

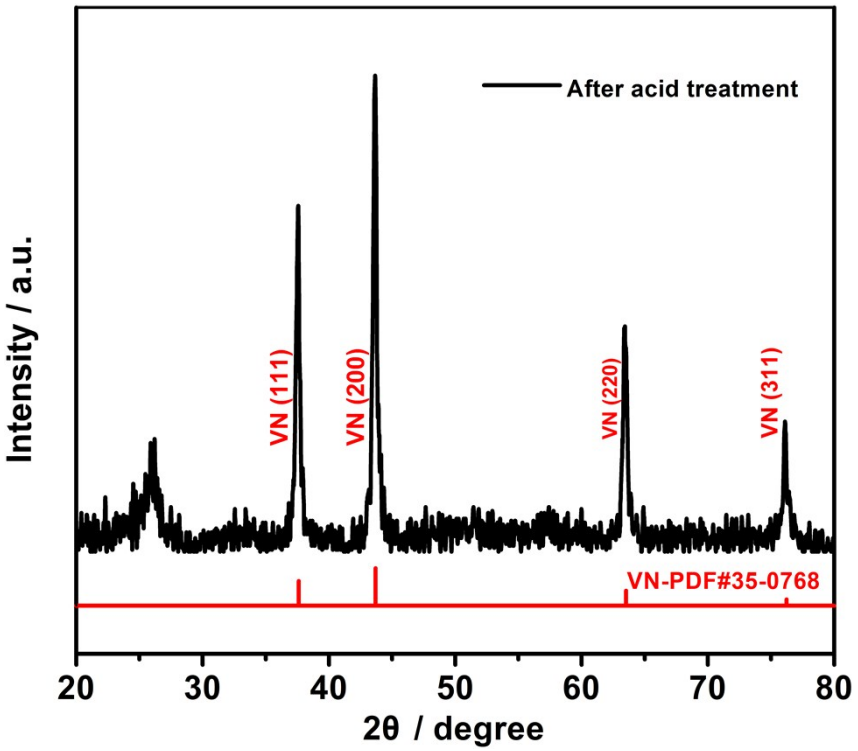

Fig. S2 XRD pattern of the NGT-V-45-900.

Table S2. The element contents for NGT-$Co_{35}V_{65}$-45-900 calculated from Fig. 3A.

Samples	Co wt. %	O wt. %	V wt. %	N wt. %	C wt. %
NGT-$Co_{35}V_{65}$-45-900	6.51	6.27	8.85	4.31	74.06
NGT-Co-45-900	8.23	6.98	0	2.13	82.66

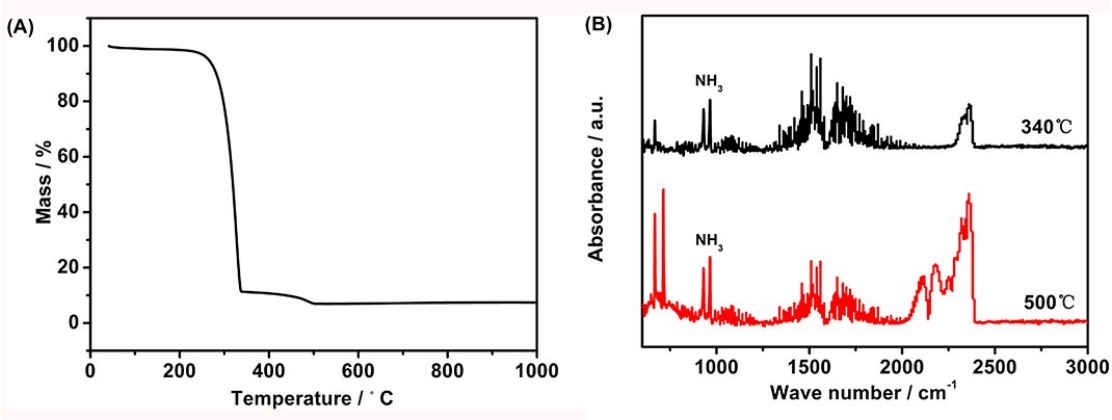

Fig. S3. Characterizations of the pyrolysis process of the precursor for synthesis of NGT-$Co_{35}V_{65}$-45-900 by TGA-IR. (A) TG curves of the precursor tested in N_2 ambient, (B) the corresponding IR spectra under 340 ^{o}C and 500 ^{o}C.

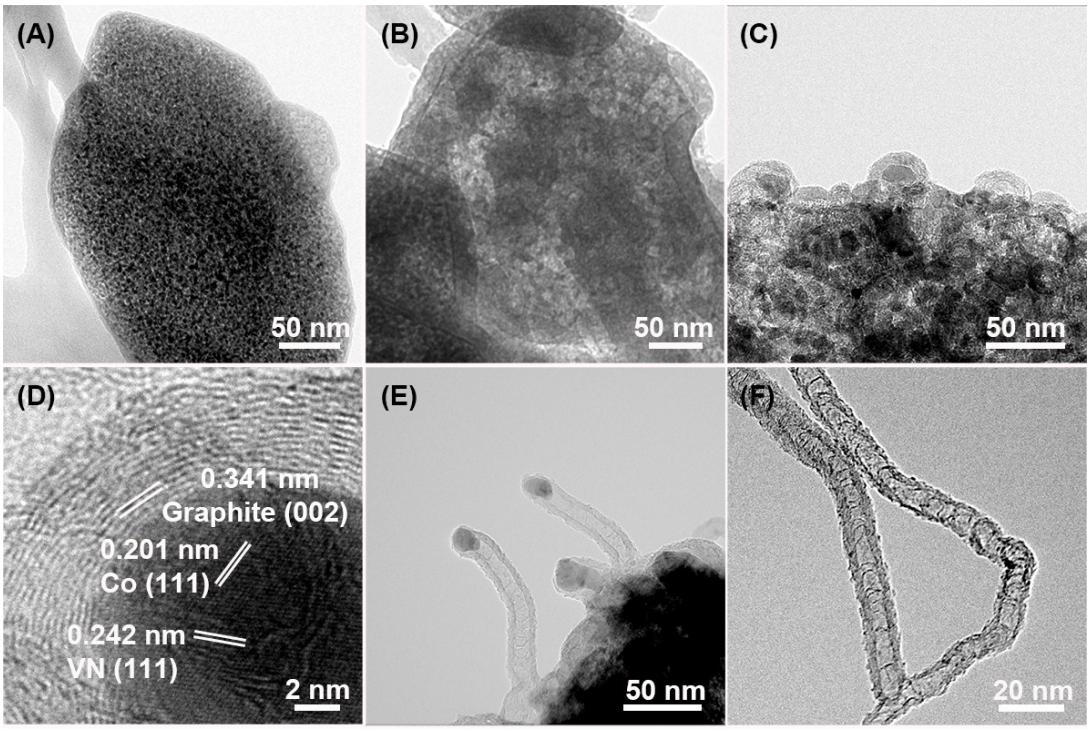

Fig. S4 TEM images of the composites derived from different carbonized temperatures: (A) NGT-$Co_{35}V_{65}$-45-340 (340 °C), (B) NGT-$Co_{35}V_{65}$-45-500 (500 °C), (C, D) NGT-$Co_{35}V_{65}$-45-600 (600 °C), (E) NGT-$Co_{35}V_{65}$-45-700 (700 °C) and (F) NGT-$Co_{35}V_{65}$-45-800 (800 °C).

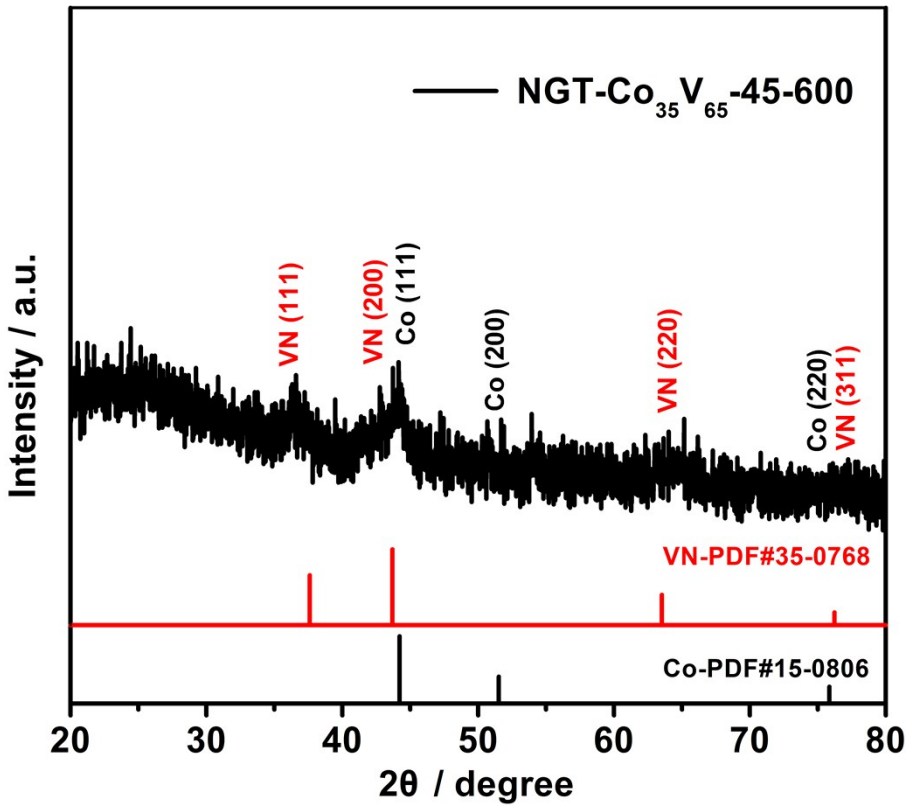

Fig. S5 XRD pattern of NGT-$Co_{35}V_{65}$-45-600.

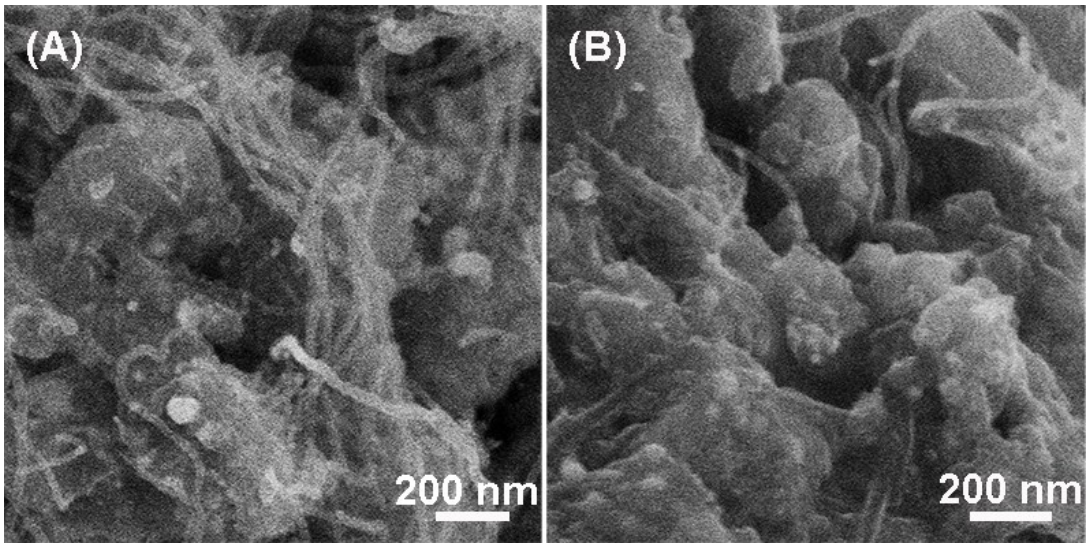

Fig. S6 SEM images of the composites derived from different atom ratio of Co:V: (A) NGT-$Co_{30}V_{70}$-45-900 (atom ratio of Co:V is 30:70) and (B) NGT-$Co_{40}V_{60}$-45-900 (atom ratio of Co:V is 40:60).

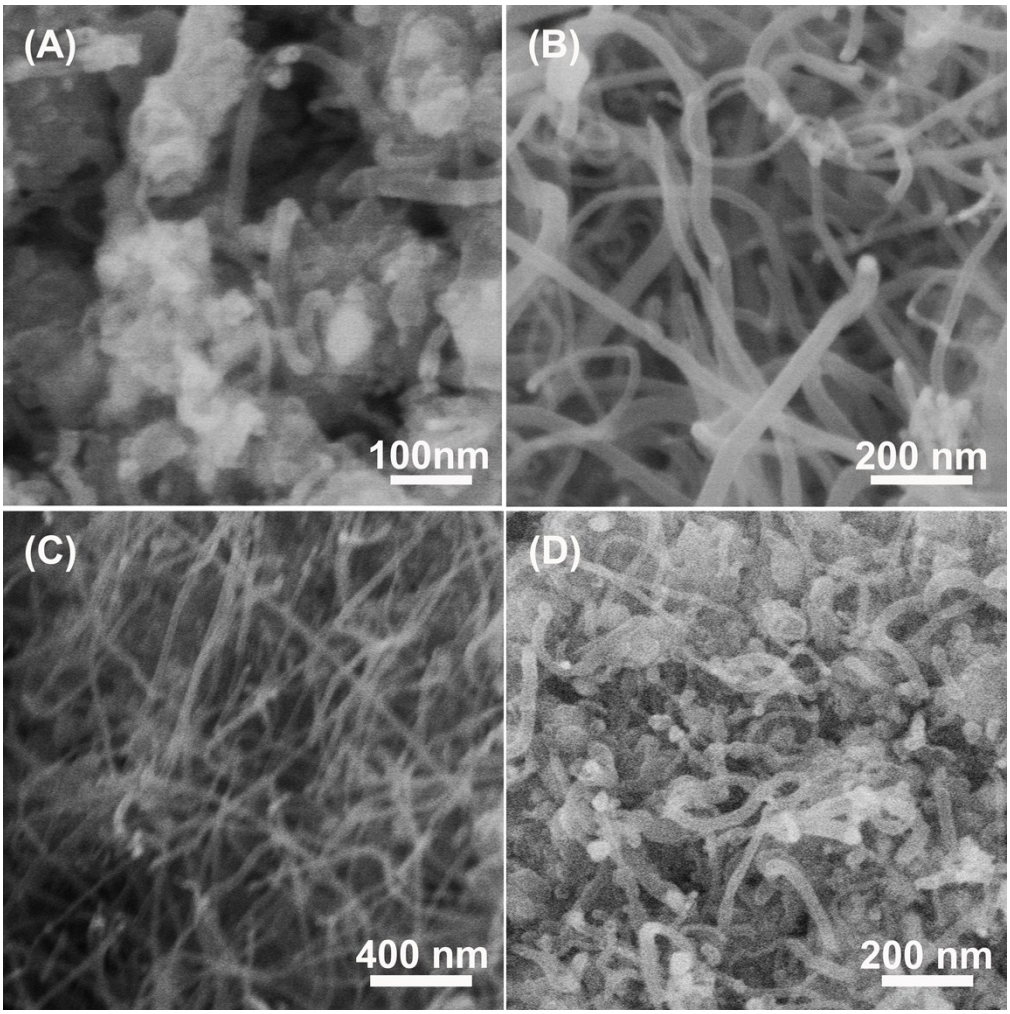

Fig. S7 SEM images of the composites derived from different dosage of melamine: (A) NGT-$Co_{35}V_{65}$-30-900 (30 mmol), (B) NGT-$Co_{35}V_{65}$-35-900 (35 mmol), (C) NGT-$Co_{35}V_{65}$-40-900 (40 mmol) and (D) NGT-$Co_{35}V_{65}$-50-900 (50 mmol).

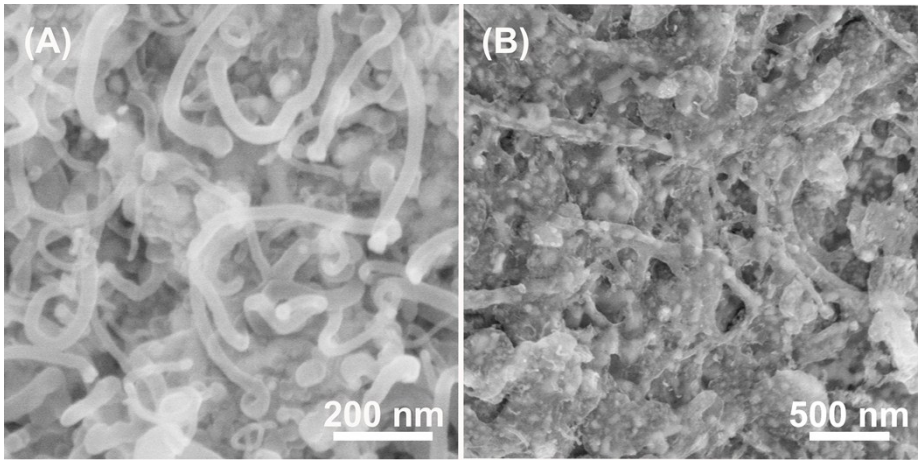

Fig. S8 SEM images of the composites derived from different carbonized temperatures: (A) NGT-$Co_{35}V_{65}$-35-800 and (B) NGT-$Co_{35}V_{65}$-35-1000.

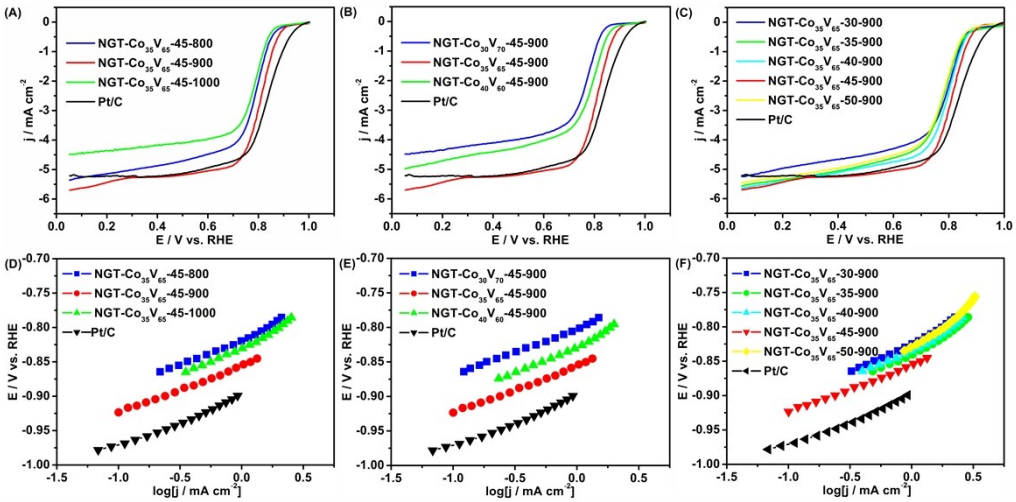

Fig. S9 (A) LSV curves and (B) Tafel plots for all the compared composites.

Table S3. ORR performances for all the compared samples.

Samples	E_{onset} (V)	$E_{1/2}$ (V)	Tafe slope (mV dec^{-1})
NGT-$Co_{35}V_{65}$-45-800	0.89	0.80	76.6
NGT-$Co_{35}V_{65}$-45-900	**0.92**	**0.81**	**66.1**
NGT-$Co_{35}V_{65}$-45-1000	0.88	0.79	86.6
NGT-$Co_{30}V_{70}$-45-900	0.87	0.77	80.4
NGT-$Co_{40}V_{60}$-45-900	0.89	0.80	71.8
NGT-$Co_{35}V_{65}$-30-900	0.89	0.80	90.2
NGT-$Co_{35}V_{65}$-35-900	0.89	0.79	89.5
NGT-$Co_{35}V_{65}$-40-900	0.90	0.80	88.0
NGT-$Co_{35}V_{65}$-50-900	0.89	0.79	102.3
NGT-V-45-900 (after acid)	0.88	0.79	70.4
NC-V-45-900	0.89	0.80	72.9
NGT-Co-45-900	0.87	0.78	79.6
Pt/C	1.00	0.85	54.2